Runx genes are direct targets of Scl/Tal1 in the yolk sac and fetal liver

Josette-Renée Landry,[1] Sarah Kinston,[1] Kathy Knezevic,[1] Marella F.T.R. de Bruijn,[2] Nicola Wilson,[1] Wade T. Nottingham,[2] Michael Peitz,[3] Frank Edenhofer,[3] John E. Pimanda,[1] Katrin Ottersbach,[1] and Berthold Göttgens[1]

[1]Department of Haematology, Cambridge Institute for Medical Research, Cambridge University, Cambridge, United Kingdom; [2]Weatherall Institute of Molecular Medicine, University of Oxford, John Radcliffe Hospital, Headington, Oxford, United Kingdom; and [3]Stem Cell Engineering Group, Institute of Reconstructive Neurobiology, LIFE & BRAIN Center, University of Bonn and Hertie Foundation, Bonn, Germany

Transcription factors such as Scl/Tal1, Lmo2, and Runx1 are essential for the development of hematopoietic stem cells (HSCs). However, the precise mechanisms by which these factors interact to form transcriptional networks, as well as the identity of the genes downstream of these regulatory cascades, remain largely unknown. To this end, we generated an *Scl*$^{-/-}$ yolk sac cell line to identify candidate Scl target genes by global expression profiling after reintroduction of a TAT-Scl fusion protein. Bioinformatics analysis resulted in the identification of 9 candidate Scl target transcription factor genes, including *Runx1* and *Runx3*. Chromatin immunoprecipitation confirmed that both *Runx* genes are direct targets of Scl in the fetal liver and that *Runx1* is also occupied by Scl in the yolk sac. Furthermore, binding of an Scl-Lmo2-Gata2 complex was demonstrated to occur on the regions flanking the conserved E-boxes of the *Runx1* loci and was shown to transactivate the *Runx1* element. Together, our data provide a key component of the transcriptional network of early hematopoiesis by identifying downstream targets of Scl that can explain key aspects of the early *Scl*$^{-/-}$ phenotype. (Blood. 2008;111:3005-3014)

© 2008 by The American Society of Hematology

Introduction

Hematopoiesis is the process by which precursor cells develop into mature blood cells of all lineages. In mouse, the yolk sac (YS) is the initial site of blood development, where large nucleated erythroblasts first arise between embryonic day 7 and 8 (E7-E8) in the blood islands. This first wave of mainly erythroid primitive hematopoiesis is followed after E9 by a second wave of YS clonogenic progenitors that are morphologically similar to fetal liver, definitive hematopoietic cells. By approximately E12 to E13, the liver, where definitive hematopoiesis is established by E11, becomes the principal hematopoietic organ.[1,2] The hematopoietic stem cells (HSCs), which colonize the fetal liver and from which all adult blood cells are derived, are thought to mainly originate from the aorta-gonad-mesonephros (AGM) region[3] with possible additional contribution from the YS.[4,5]

Several transcription factors have been shown to be indispensable for normal YS hematopoiesis. The *Scl* gene (also known as *Tal1*), which encodes a basic helix-loop-helix (bHLH) transcription factor, is essential for YS and fetal liver hematopoiesis.[6,7] Embryos lacking Scl are pale and growth retarded and do not survive beyond E9.5. In addition to the complete absence of hematopoietic cells, *Scl* null embryos fail to properly remodel the YS vasculature, suggesting a role for *Scl* in angiogenesis.[8] Mice lacking Lmo2, a member of the LIM-only zinc finger protein family and an interacting partner of Scl, have a very similar phenotype,[9,10] consistent with the notion that early hematopoietic development critically depends on a protein complex containing Scl and Lmo2. Recent work in zebrafish[11] indeed suggests that *lmo2* and *scl* function together at the level of the hemangioblast where they play a key role in the initiation of blood and vascular transcriptional programs.

Together with bHLH class I proteins, such as E47, Scl binds DNA as a heterodimer, to the E-box sequence motif CANNTG. In addition to its bHLH DNA-binding partners, Scl can interact with various proteins, including Lmo2 in multimeric complexes. In erythroid cells, Scl and Lmo2 have been shown to form a complex with E2A, Gata1, and Ldb1[12] while pairing in a similar aggregate with Gata2 instead of Gata1 in multipotent hematopoietic progenitors.[13] As part of such protein complexes, Scl and Lmo2 have been found to regulate a handful of genes, including *c-kit*[14] and α-*globin*[15] in different hematopoietic lineages. However, to date, other than one study in T-ALL cells,[16] no systematic approach has been taken to interrogate potential target genes of Scl on a whole genome basis, especially not at early developmental time points where Scl function is critical.

We have now generated a novel *Scl*$^{-/-}$ YS cell line to identify on a genomic scale by microarray analysis, genes that are up-regulated after the reintroduction of Scl protein. The binding of Scl to these potential target genes was then confirmed using chromatin immunoprecipitation (ChIP). Previous work by our group had established that *Runx1* is indirectly linked to the Scl transcriptional network in the AGM through their common association with the SMAD signaling pathway.[17] Here, we report that Scl directly binds and regulates *Runx1* in the YS as well as *Runx1* and *Runx3* in the fetal liver.

Methods

Establishment of YS cell line

Yolk sacs were isolated from E9.5 *Scl*$^{-/-}$ embryos[6] as well as from wild-type controls. Cells were disaggregated with a 26-gauge needle and

transferred into a 6-well dish where they were cultured in hemangioblast growth medium,[18] composed of Iscove modified Dulbecco medium with 10% fetal calf serum, 10% horse serum, vascular endothelial growth factor 10 ng/mL, stem cell factor (SCF) 20 ng/mL, interleukin-6 10 ng/mL, monothioglycerol, Penn/Strep. To confirm the genotype of the obtained YS cells, polymerase chain reaction (PCR) was performed on the remainder of the embryos. Briefly, an amplicon of 596 bp was obtained from the targeted allele using a Pgk poly a sense oligo (gaa ggg tga gaa cag agt acc tac) within the neo cassette and a reverse primer in *Scl* (GCATGCTCAAGGCTGCTG ACTTGG), whereas a 424 bp amplicon was obtained from wild-type mice using a sense *Scl* oligo (GTT TTG GTC TAG AGT TTG TGA GCC) and the same antisense *Scl* oligo.

After 1 day of culture, adherent and suspension cells from each well were individually transfected with the plasmid pUCIn-wt,[19] which encodes the entire genome of SV40 except for a deletion at the origin of replication, in the presence of the Effectene reagent (Qiagen, Crawley, United Kingdom). After transfection, adherent and suspension cells from each well were combined and passaged on a weekly basis. After 28 days, actively growing adherent cells with an approximately 12-hour doubling time were present in 2 of the *Scl*^{−/−} wells. These cells were expanded as the YS1 and YS2 cell lines and frozen down. On recovery, YS1 and YS2 cells were transferred into RPMI-10% fetal calf serum media and kept in continuous culture for 8.5 months with no apparent change in morphology or growth rate.

Characterization of cell line

Matrigel (BD Becton Dickinson, Oxford, United Kingdom) was prepared as specified by the manufacturer and allowed to polymerize on 24-well plates at 37°C for 30 minutes. YS1, YS2, and RM26 (murine mesenchymal stem cell line) cells were plated at a density of 2×10^4 cells/well and incubated at 37°C for 3 hours, at which time the initiation of tube formation could be seen. Total RNA was prepared using QIAGEN RNeasy midi kit. Primers, spanning at least one intron, were designed for 45 mouse genes (primer sequences available on request). RT-PCR was performed with each primer pair on total RNA from YS1 and YS2 with negative water control and whole E11.5 embryo total RNA as positive control. Images in Figure 1 were acquired using a Pixera Pro 150ES digital camera (Pixera, Los Gatos, CA) attached to a Nikon SM7800 microscope (Nikon, Kingston upon Thames, United Kingdom). ImagePro Express version 4.5 (Images Processing Solutions, North Reading, MA) was used for acquisition of images, which were processed using Adobe Photoshop (Adobe Systems, San Jose, CA). Images in Figure 5 were acquired on an Axioskop 2 widefield microscope (Carl Zeiss, Jena, Germany) with a 5×/0.15 numeric aperture objective by an Axiocam MRc5 camera (Carl Zeiss), and were processed by Axiovision v43 (Carl Zeiss) and Adobe Photoshop v8 (Adobe Systems) software. Mounting/imaging medium was Hydromount (VWR International, Lutterworth, United Kingdom). In situ hybridizations were performed as described.[20]

Reintroduction of wild-type and ΔbHLH SCL by protein transduction

Full-length SCL and ΔbHLH SCL proteins were directly delivered into cells by protein transduction. For that purpose, fusion proteins were generated consisting of SCL and the protein transduction peptide TAT. A murine Scl encoding fragment was generated using primers 5′FL4TAT (ataaaagcttaatgacggagcggccgccgagcgag) and 3′4TAT (aattctcgagtcac-cgggggccagccccatcagc). This fragment was cloned into the *Hin*dIII and *Xho*I restrictions sites of pTRiEx,[21] resulting in pTRiEx-HT-SCL. To obtain pTRiEx-HT-ΔbHLH SCL, a C-terminal truncated version of Scl lacking the basic helix-loop-helix (bHLH) domain, was amplified using 5′FL4TAT and Del_bHLH_rev (atactcgagttattactcatatggggagggcctcct) and cloned as described for the wild-type construct.

Expression and purification of recombinant fusion proteins were performed as described.[21] Briefly, overexpression was induced by isopropyl-b-D-thiogalactopyranoside (IPTG), and after an additional incubation of 3 to 4 hours at 37°C, cells were harvested, frozen in dry ice-ethanol, and resuspended in lysis buffer [100 mM NaH_2PO_4, 10 mM Tris (pH 8.0), 300 mM NaCl, 10 mM imidazole]. Lysates were cleared by incubation with

lysozyme (Sigma-Aldrich, Dorset, United Kingdom) and benzonase (Nova-gen, Darmstadt, Germany) and centrifugation for 25 minutes at 30 000*g* at 4°C. Ni-NTA slurry (QIAGEN) was used for column affinity purification of the His-tagged recombinant protein. Recombinant protein was eluted [100 mM NaH_2PO_4, 10 mM Tris (pH 8.0) 300 mM NaCl, 250 mM imidazole] and dialyzed against phosphate-buffered saline (PBS) for immediate use. Protein concentrations were measured using Bradford reagents (Sigma-Aldrich). For protein transductions, 5×10^5 YS1 cells were seeded on 6-cm plates. After 24 hours, TAT-SCL protein was added to a final concentration of 2 μM. Western blots were performed using standard protocols.

Microarray hybridization and computation analysis

Total RNA was isolated from YS1 cells 7 hours after transduction according to the manufacturer's protocol (QIAGEN); 20μg of extracted RNA was sent to NimbleGen (Reykjavik, Iceland) to be hybridized unto their mouse 60mer catalog design of mouse build 5 from UCSC (34 062 genes at a minimum of 11 probes per gene). GO and KEGG terms associated with the overexpressed transcripts were identified using IDconverter (http://idconverter.bioinfo.cnio.es/). Bioinformatic searches for E-boxes were performed using CoMoDis,[22] using the following parameters: N0, N1, and N2 degrees of extended TFBS conservation and only considering motifs present in mouse-dog or mouse-opossum alignments, within 20 kb of the genes. The microarray experiments have been deposited in ArrayExpress under the accession number E-TABM-397 (http://www.ebi.ac.uk/microarray-as/aer/entry).

Chromatin immunoprecipitation

ChIP assays were performed as previously described.[23] Briefly, 416B cells were treated with formaldehyde and the cross-linked chromatin was sonicated to obtain fragments of 200 bp averaged size; 75 YSs were dissected from day 8.5 wild-type embryos and treated with collagenase, whereas 60 fetal livers were dissected from day 11.5 embryos and disrupted by pipetting before cross-linking. Immunoprecipitations were performed with an Scl antibody (provided by C. Porcher, Weatherall Institute of Molecular Medicine, Oxford, United Kingdom) and anti-Lmo2 (AF2726, R&D Systems, Abingdon, United Kingdom), −Gata2 (SC-9008X, Santa Cruz Biotechnology, Santa Cruz, CA), −E47 (SC-763X, Santa Cruz Biotechnology) as well as an anti-acetyl histone H3 antibody (06-599, Upstate Biotechnology, Watford, United Kingdom). Enrichment was measured by real-time PCR using Primer 3 designed oligonucleotides flanking the computationally identified E boxes. Dissociation curves were run to detect nonspecific amplification, and it was determined that single products were amplified in each reaction. The fold enrichment was calculated using standard curves, and results were expressed relative to the levels obtained with a rabbit IgG antibody.

Transactivation assay

Cos cells were transfected by electroporation with a *Runx1* candidate element luciferase construct alone (pGL3P + 23[24]) or in combination with the after expression constructs: pEFBOS MycT LMO2, pEFBOS MycT Gata2, pEFBOS Flag SCL, pEFBOS Ldb1 and pcDNA3 Myc E47. The Lmo2 and Gata2 expression plasmids were kindly provided by T. H. Rabbits (Leeds Institute of Molecular Medicine, University of Leeds, Leeds, United Kingdom), the Scl by C. G. Begley (The Walter and Eliza Hall Institute of Medical Research, University of Melbourne, Australia), the E47 by Y. Saga (National Institute of Genetics, Yata, Japan), and the Ldb1 plasmid by C. Porcher. Each transfection was performed on at least 2 different days in triplicate, and an equivalent quantity of DNA was transfected using the empty vectors pcDNA3 and pEFBOS as controls when necessary.

Results

Generation of *Scl*^{−/−} YS cell line

To identify potential Scl target genes, we created a cell line using YSs obtained from embryonic day 9.5 *Scl*^{−/−} mice to investigate

Figure 1. Characterization of an *Scl*⁻/⁻ YS cell line.
(A) Comparison of day 9.5 *Scl*⁻/⁻ (left) and wild-type (right) embryos. (B) Genotyping PCR of Scl⁺/⁻ progeny and derived cell lines, where 1, 9, 10, 11, YS1, and YS2 are homozygous null. (C) Morphology of YS1 (i) and RM26 (ii) cells. (D) Differentiation of cells on matrigel YS1 plated on matrigel (i) and RM26 plated on matrigel (ii). RM 26 is a murine mesenchymal stem cell line with known endothelial differential potential.[72]
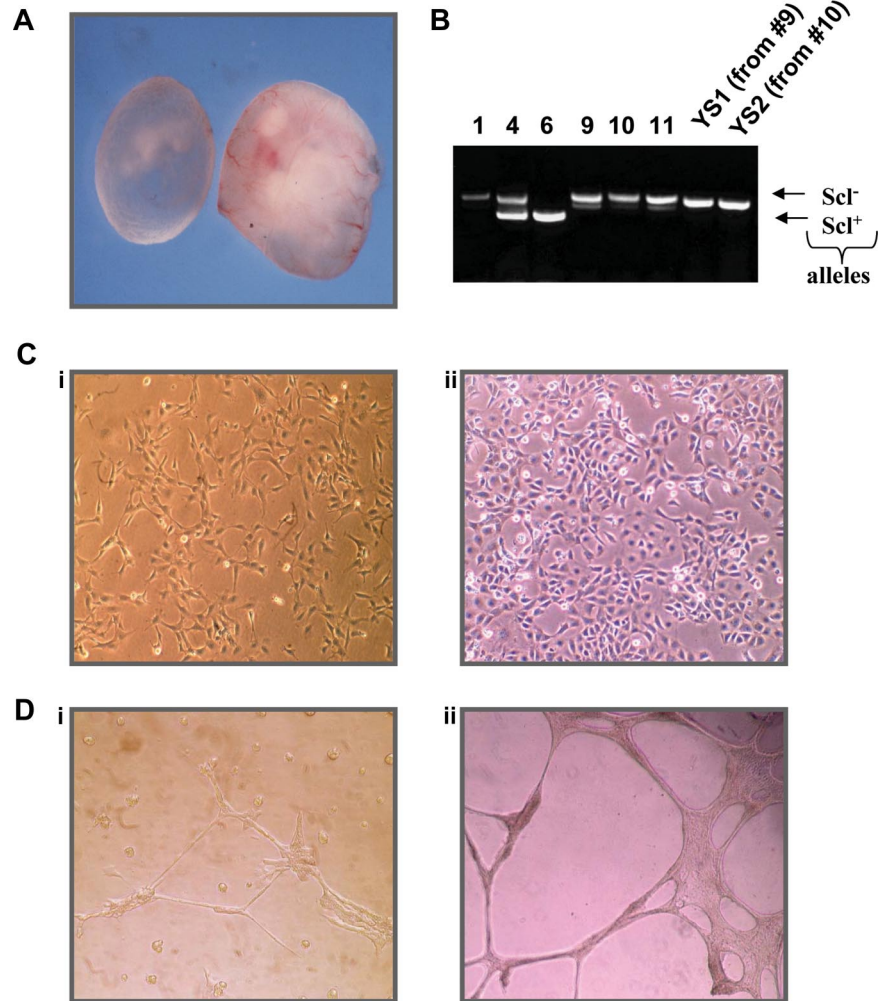
differences in gene expression after reintroduction of SCL. As shown in Figure 1A, *Scl*-null embryos are discernible by eye as they are pale in appearance and growth retarded presumably as a consequence of their anemia and vascular defects. We isolated YSs from homozygous null *Scl* embryos and transfected disaggregated cells with an SV40 plasmid to generate immortalized cell lines. PCR genotyping was performed on the remainder of the embryo to confirm the genotype (Figure 1B).

After 1 month in culture, cells from 2 independent *Scl*⁻/⁻ YSs (9 and 10) had expanded and become immortalized and were single-cell cloned. The 2 resulting cell lines (named YS1 and YS2) exhibited the morphologic characteristics of endothelial cells, growing as a cobblestone-like adherent monolayer with some cytoplasmic interdigitation and overlap (Figure 1C). To confirm the endothelial characteristics, cells were cultured on basement membrane matrix (Matrigel) coated plates as shown in Figure 1D. YS1 grown on plastic displayed a cobblestone morphology, whereas their incubation on Matrigel resulted in cell elongation and the formation of tube-like structures, reminiscent of endothelial cells. Similar results were obtained for YS2 cells (data not shown).

To further characterize the 2 cell lines, we examined the mRNA expression of hematopoietic and endothelial markers by reverse transcription (RT)-PCR (Table S1, available on the *Blood* website; see the Supplemental Materials link at the top of the online article). Both YS1 and YS2 cells expressed mRNA of many endothelial markers, such as fetal liver kinase 1 (*Flk1*), thrombomodulin, and *Cd34*. However, neither cell line expressed the hematopoietic

markers *Pu.1* and *Vav* nor the mesodermal marker brachyury, consistent with an endothelial phenotype.

Expression profile of *Scl* ⁻/⁻ YS cell line after reintroduction of Scl

To assess transcriptional differences in gene expression after SCL reintroduction in YS1 cells, we performed gene-expression profiling analysis using cDNA microarrays. Because it was difficult to maintain Scl expression after transfection of an Scl expression plasmid (S.K., B.G., unpublished results, February 2004), we used a TAT fusion protein transduction system to introduce Scl proteins into the cells directly, which has been shown to permit protein transduction into a variety of cell lines and primary cells.[21,25-27] We therefore generated expression vectors for the production of His-tagged full-length TAT-Scl fusion protein as well as a C-terminally truncated form lacking the bHLH domain (TAT-Scl ΔbHLH, Figure 2A). This truncated version of Scl is unable to bind DNA, cannot heterodimerize with E2A proteins, and importantly does not rescue the early hematopoietic phenotype of *Scl*⁻/⁻ ES cells.[28] Expression and purification of recombinant proteins were performed as described previously,[21] with only minor modifications (see "Reintroduction of wild-type and ΔbHLH SCL by protein transduction").

After IPTG induction and affinity purification of recombinant protein using Ni²⁺-affinity chromatography, soluble full-length and truncated recombinant Scl protein were routinely obtained (Figure

A

TAT-SCL [H | TAT | SCL | HLH]

TAT- ΔBHLH SCL [H | TAT | SCL Δ BHLH]

B

C

i

kD   M -I +I P SN FT W1 W2 E1 E2

62 —
48 —
33 —

ii

48 —

M   + PBS   + TAT-SCL

66 —
45 —
31 —
22 —

Figure 2. Reintroduction of SCL using TAT-mediated protein transduction. (A) Depiction of full-length and truncated TAT-SCL fusion proteins. (B) (i) Coomassie staining and (ii) Western blot (anti-His) of bacterially expressed TAT-SCL. M indicates marker; −I, before induction; +, induction; IPTG, 1 hour; P, pellet; SN, supernatant; W1,2, wash with 10 mM imidazole; E1,2, 250 mM. (C) Western blot of YS1 cells with anti-SCL after transduction with recombinant TAT-SCL protein.

2B; data not shown). After dialysis against PBS, the recombinant protein was used to transduce YS1 cells and could be detected using a polyclonal antibody against Scl in cells transduced with Scl protein but not control cells incubated with PBS alone (Figure 2C).

Total RNA was then isolated from YS1 cells transduced with wild-type Scl protein or treated with PBS alone and analyzed by microarray expression profiling using the NimbleGen mouse 60mer expression microarray platform, which detects differential gene-expression patterns between a test and control sample (eg, cell transduced with Scl protein dissolved in PBS vs PBS alone). A total of 2 biologic replicates transduced with full-length Scl and 2 replicates transduced with the ΔbHLH Scl protein were analyzed in this way (Figure 3A). Differences in gene-expression patterns between cells transduced with the wild-type or truncated SCL were then compared, using the strategy outline in Figure 3B. Genes were defined as up-regulated if they matched the following criteria: (1) their expression varied by more than 1.5-fold in cells transduced with wild-type Scl versus PBS controls, and (2) their expression did not vary (< 1.5) in cells transduced with the mutant

ΔbHLH Scl versus PBS controls. By using these cut-offs, our analysis revealed 160 transcripts, corresponding to 124 genes showing up-regulated expression after reintroduction of Scl (Table S2). It is worth noting that the expression of *Scl* could not increase after transduction as the cells were homozygous null for Scl and no expression plasmid for Scl was transduced, only the TAT-fused protein.

Many of the most highly induced genes were annotated to be part of the interferon response and related immune-response pathways, presumably because the recombinant proteins contained endotoxins and related *Escherichia coli* contaminants. To account for genes whose differential expression might simply be the result of cellular stress or the consequence of immune response after the use of a bacterially produced recombinant protein, we therefore tabulated a list of lipopolysaccharide-induced genes from the literature.[29-34] In addition to lipopolysaccharide-induced genes, we also removed from our list genes with a known immune function (gene ontology terms GO:0006955 or KEGG term mmu04650). This parsing reduced our list of candidates whose expression is influenced by Scl to 90 genes. Our own particular interest lies in the delineation of transcriptional networks that control early blood development.[17,35] We therefore further narrowed our candidate Scl target gene list to those with DNA binding or transcription factor activity (GO:0003677 and GO:0003700) and manually curated the list to remove false-positives. As shown in Figure 3B, this left us with 15 potential Scl target genes that met these stringent criteria.

Identification of Scl target genes

To assess whether the up-regulated transcription factor genes found in this study could be direct targets of Scl, we screened their gene loci for the presence of E-boxes conserved between human, mouse, dog, and opossum. We identified 361 CANNTG, conserved between human-mouse-dog, within 20 kb of 12 of the 15 candidate target genes. Using an increased conservation stringency, by limiting the hits to only those conserved in opossum and by modifying the extent of conservation by including the 2 flanking nucleotides (n2), we reduced our list of candidate target sequences to 121 E-boxes localized to 9 genes, which are listed in Table 1.

A

TAT-SCL+/- bHLH   PBS

RNA   RNA

label 1   label 2

4 x Microarray

Hybridization

B

Inclusion criteria	Gene Number
	34062
Expression variation: wild-type SCL >1.5 x ΔbHLH SCL <1.5 x	
	124
Non LPS-induced and no immune function	
	90
GO annotation for TF, DNA binding	
	15
Presence of E-boxes conserved between mouse-opossum	
	9

Figure 3. Schematic depicting the strategy for the transcriptional profiles of an SCL⁻/⁻ YS cell line after reintroduction of Scl. (A) Outline of protein transduction/expression profiling strategy. (B) Diagram showing the stepwise bioinformatic filtering of candidate target genes.

Table 1. Transcription factors overexpressed after transduction of SCL protein into the YS1 *Scl*^{-/-} cell line

	Conserved E boxes				
	Opossum			Dog	
Gene	N0	N1	N2	N0	Gene description
Creb3l1	12	5	3	23	CAMP responsive element binding protein 3-like 1
Dnajc1	16	9	6	19	DnaJ (Hsp40) homolog, subfamily C, member 1
Hivep2	7	2	1	9	HIV type I enhancer binding protein 2
Irx1	14	8	6	14	Iroquois related homeobox 1 (Drosophila)
Mll1	12	9	6	13	Myeloid/lymphoid or mixed-lineage leukemia 1
Nfib	78	47	31	100	Nuclear factor I/B
Runx1	25	11	7	58	Runt related transcription factor 1
Runx3	4	N/A	2	N/A	Runt related transcription factor 3
Zfhx1b	93	65	59	115	Zinc finger homeobox 1b

Names of genes shown to the left are followed by the number of conserved E boxes as determined by CoMoDis[22] (with N0, N1, and N2 extended conservation criteria) and short gene descriptions.

This list included the *Runx1* and *Runx3* transcription factors. Runx1 was known to be essential for the development of definitive hematopoietic cells in the murine YS and fetal liver,[36,37] whereas Runx3 had been shown to be necessary for hematopoietic development in the zebrafish.[38] Given their known function in early hematopoiesis, we were keen to establish whether they might be direct target genes of Scl.

To determine whether computationally identified conserved E-boxes in the *Runx1* and *Runx3* loci were actually bound by Scl in vivo, we performed chromatin immunoprecipitations using an anti-Scl antibody in the myeloid progenitor 416B cell line. Immunoprecipitated chromatin samples were then analyzed by quantitative real-time PCR with the use of primers specific for the regions containing the conserved motifs. As shown in Figure 4A, there are 7 conserved E boxes in the *Runx1* locus (using the strict N2 definition outlined above). The first intronic site

(#2) present downstream of the distal P1 promoter shows an enrichment level of more than 150-fold in an anti-Scl immuno-precipitate of 416B cells compared with neighboring sites (Figure 4A; Figure S1). Equivalent analysis of the *Runx3* gene locus showed that the distal promoter of *Runx3* is also occupied by Scl and displays a 16-fold enrichment in material from 416B cells (Figure 4B; Figure S1).

Taken together, the expression profiling and ChIP assays suggested that both *Runx1* and *Runx3* are direct target genes of Scl. However, to validate this hypothesis, it was important to demonstrate Scl binding to the respective *Runx* elements in vivo in primary tissues. We therefore dissected 75 YSs from E8.5 embryos and 60 fetal livers from E11.5 embryos and repeated the ChIP assays using an antibody against Scl. Because of the paucity of the material, we only assessed those regions in *Runx1* and *Runx3* for which the initial screening, using 416B material,
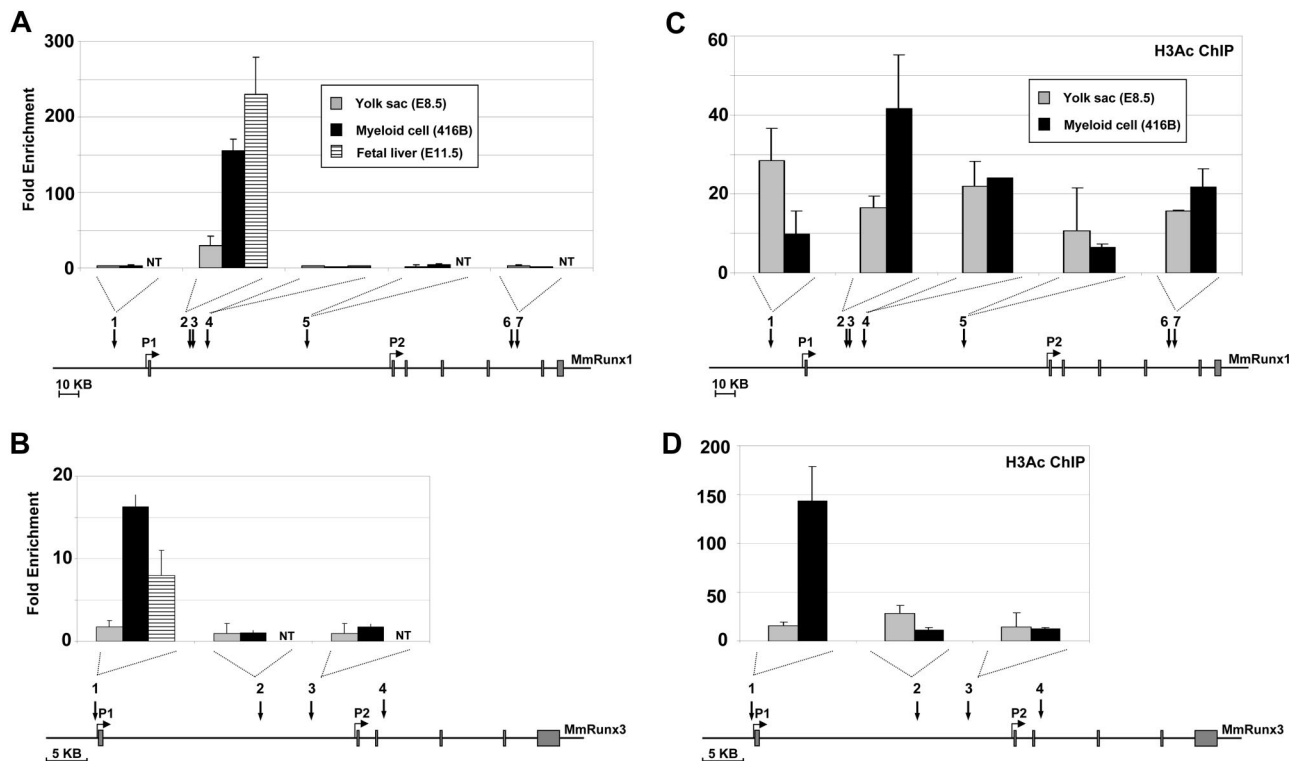
Figure 4. Scl occupies the *Runx3* promoter and a *Runx1* candidate enhancer in vivo. Real-time PCR analysis of ChIP performed with anti Scl (A,B) and antiacetylated histone 3 (C,D) antibodies. The y-axis represents enrichment over that obtained with a rabbit IgG antibody. The x-axis represents the coordinates at the mouse Runx1 (A,C) and Runx3 (B,D) gene loci where the conserved E-boxes are depicted by numbered arrows. NT indicates not tested. Error bars represent SD.

indicated a positive enrichment level. Our results shown in Figure 4A,B demonstrate that *Runx1* candidate 2 is enriched more than 25-fold in the YS Scl IP and more than 230-fold in the fetal liver. The proximal promoter of *Runx3* displays a marginal enrichment over that obtained with an unspecific IgG antibody in YS and was 8-fold enriched in fetal liver. We also investigated the chromatin profile of the candidate *Runx1* and *Runx3* elements by analyzing ChIP material obtained with an anti-acetyl histone H3 antibody. Our data, shown in Figure 4C,D show moderate to high levels of acetylation at all regions tested in the *Runx1* locus in both E8.5 YS and 416B myeloid cells with the highest levels of enrichment seen at the intron 1 region also bound by Scl. For the *Runx3* gene locus, high levels of histone acetylation were observed in the promoter in 416B cells but much lower levels in the YS, paralleling the Scl binding data shown in Figure 4B.

To further validate Runx1 and Runx3 as direct Scl target genes, high resolution expression studies were performed on E8.5 and E11.5 mouse embryo sections. RNA in situ hybridization demonstrated strong Scl expression in the majority of cells contained within E8.5 YS blood islands as well as E11.5 fetal liver cells. Strong Runx1 expression was seen in a subset of E8.5 blood island and E11.5 fetal liver cells. Runx3 was also detected in a subset of E11.5 fetal liver cells in agreement with previously published immunohistochemistry data,[39] yet no specific staining could be detected in E8.5 blood islands. At E11.5, all 3 genes were also expressed in specific nonhematopoietic tissues, such as the developing spinal cord (Scl), tips of the urogenital ridges (Runx1) and dorsal root ganglia (Runx3). Expression levels were also determined by real-time PCR confirming the very low expression of Runx 3 in E8.5 YS (> 15 times less than Runx1, Figure S3). To investigate coexpression of Scl, Runx1, and Runx3 during adult hematopoiesis, we queried the 79 human tissues profiled by the Genomic Foundation of Novartis GNF SymAtlas (http://symatlas.gnf.org), version 1.2.4 online server. Importantly, all 3 genes were expressed at more than 10-fold over median in human CD34+ cells (Figure S5), which is entirely consistent with our data showing occupancy of both the Runx1 and Runx3 elements in fetal liver and a myeloid progenitor cell line.

To provide further evidence of Runx1 being a target gene of Scl during YS hematopoiesis, mRNA levels for *Scl*, *Runx1*, and *Runx3* were determined by real-time PCR using RNA samples prepared from E8.5 $Scl^{+/+}$, $Scl^{+/-}$, and $Scl^{-/-}$ YSs (Figure 5C). This analysis demonstrated that $Scl^{+/-}$ YSs, which showed exactly half the wild-type amount of Scl message, also displayed a near 50% drop in *Runx1* mRNA levels, whereas *Runx3* remained unchanged. *Runx1* levels dropped further in $Scl^{-/-}$ YSs, whereas *Runx3* increased slightly from its very low basal level of expression in normal YSs (see Figure 5A). However, $Scl^{-/-}$ YSs do not contain any hematopoietic cells, suggesting that the more meaningful comparisons are between wild-type and $Scl^{+/-}$ as they contain similar populations of cells. Importantly, the tissue-specific binding of Scl to *Runx1* and *Runx3* elements correlates well with *Runx1/3* expression patterns, with strong binding seen to both gene loci in fetal liver but only to the *Runx1* element in the YS. Taken together, these results identified *Runx* genes as direct Scl target genes in embryonic tissue.

Runx1 is regulated by an Scl/Lmo2/Gata2 complex

To begin to understand how these newly identified Scl-bound *Runx1* and *Runx3* elements may be regulated, we performed multiple sequence alignments to identify conserved transcription
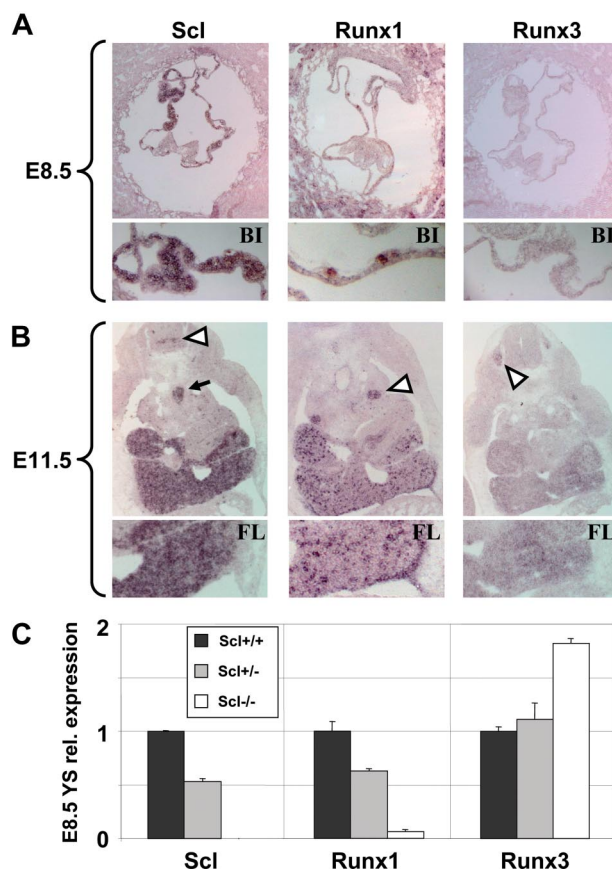

Figure 5. Expression of *Scl*, *Runx1*, and *Runx3* at E8.5 and E9.5 of mouse embryonic development. Transverse sections of E8.5 (A) and E11.5 (B) mouse embryos hybridized to digoxigenin labeled antisense RNA probes for *Scl*, *Runx1*, and *Runx3*. (A) E8.5 whole embryo transverse sections (top panels) and close-up views of YS blood islands (bottom panels). *Scl* and *Runx1* were specifically expressed in YS blood islands, whereas no specific expression was detected for *Runx3*. (B) E11.5 whole embryo transverse sections (top panels) and close-up views of fetal liver (bottom panels). *Scl*, *Runx1*, and *Runx3* were all specifically expressed in the fetal liver. *Scl* was also expressed in the dorsal aorta (◁) and developing spinal cord (→), *Runx1* in the tips of the urogenital ridges (◁), and *Runx3* in the developing dorsal root ganglia (◁). (C) Quantitative RT-PCR analysis for *Scl*, *Runx1*, and *Runx3* expression in $Scl^{+/+}$, $Scl^{+/-}$, and $Scl^{-/-}$ E8.5 YSs. Expression was normalized against β-actin and expression in the $Scl^{+/+}$ E8.5 yolks sacs was set as 1 for each gene. Error bars represent SD.

factor binding sites. As shown in Figure 6A, the *Runx1* candidate element contains several Ets sites as well as 2 E-boxes, 1 GATA and 1 Runx binding site that are conserved between eutherian mammals and marsupials. Some of these transcription factor binding sites, but not the GATA site, are also present in the P1 promoter of *Runx3* (Figure 6B). The presence of conserved E-boxes in the vicinity to a conserved GATA site suggested that the Runx1 element might be controlled by an Scl/Lmo2/Gata multiprotein complex. To investigate this possibility, we performed ChIP for Scl, Lmo2, E47, and Gata2 proteins to determine whether these factors occupied the element in vivo. Real-time PCR analysis demonstrated that, in addition to Scl, the *Runx1* element is bound by Lmo2 and Gata2 (Figures 7A, S2). It is worth noting that the differences in the enrichment levels obtained are likely due to variations in the efficiency of the antibodies, which may reflect the accessibility of the proteins or epitopes in the complex.

To assess whether these transcription factors were sufficient to modulate the activity of the *Runx1* element, we performed transactivation assays. We transiently cotransfected Cos cells

A

B
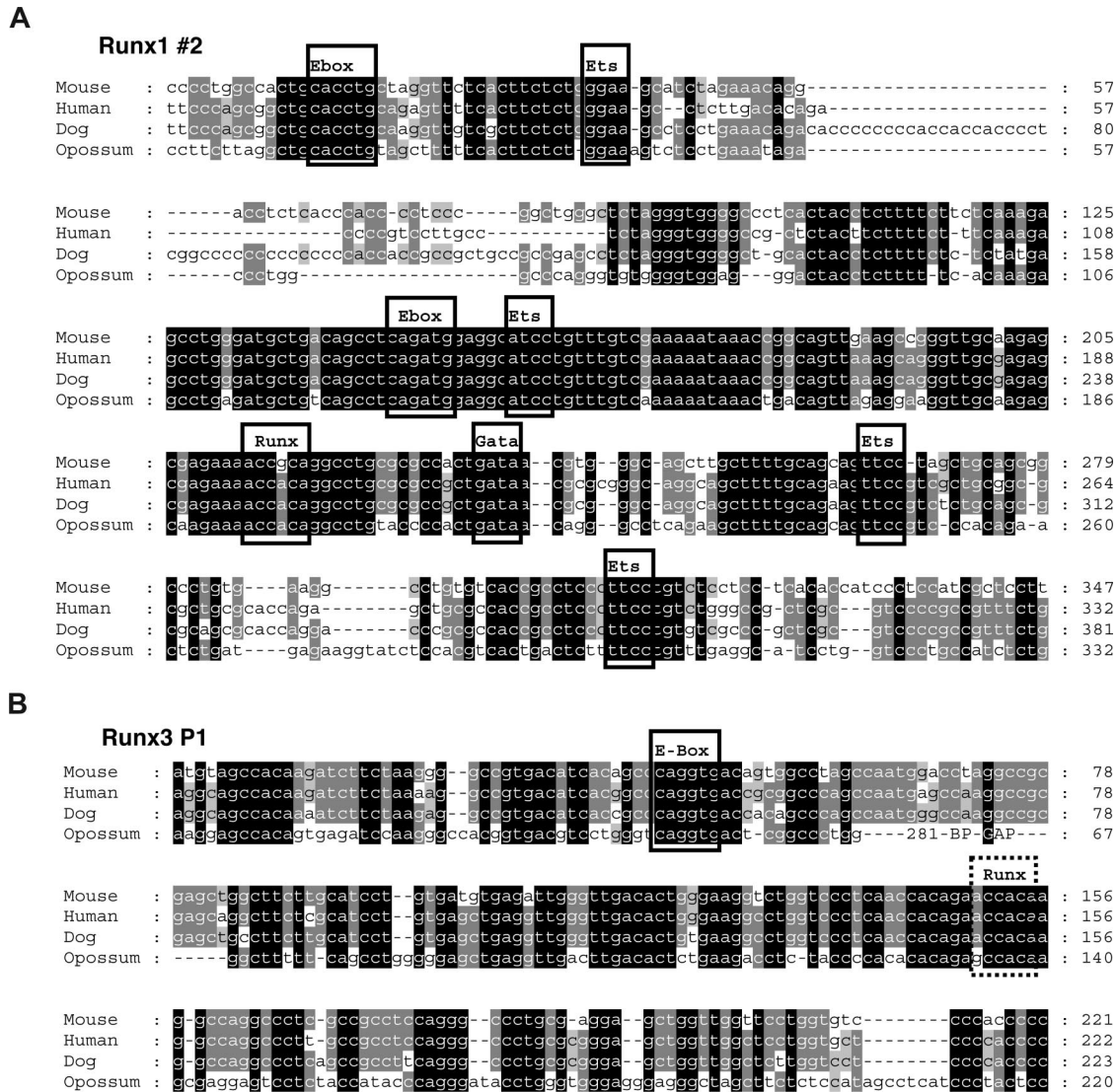
Figure 6. Conserved E-boxes and GATA sites are present in *Runx1* and *Runx3*. Multiple sequence alignments of the region flanking the conserved E-boxes in *Runx1* (A) and *Runx3* (B). Predicted conserved transcription factor binding sites are boxed when present in all 4 species and marked by a dashed box when only conserved in eutherian mammals.

with a *Runx1* luciferase reporter construct containing the candidate element *2* in conjunction with plasmids encoding Scl, Lmo2, E47, Ldb1, and Gata2. As shown in Figure 7B, the activity of *Runx1* reporter plasmid was increased 1.5-fold when cotransfected with a Gata2 expression construct, whereas cotransfection of Scl, Lmo2, Ldb1, and E47 had no effect. Importantly, addition of the 5 transcription factors together increased reporter gene activity further to 4.5-fold, indicating that Scl, E47, Ldb1, and Lmo2 contribute to full transactivation only when complexed with Gata2.

Discussion

Transcriptional regulation is a key factor controlling the formation and subsequent behavior of HSCs.[40-42] Both gain- and loss-of-function studies have demonstrated that transcription factors are some of the most powerful regulators controlling the specification, self-renewal, and differentiation of HSCs (eg, Scl, Gata2, Lmo2, Pu.1). The importance of transcriptional regulation in both normal

and leukemic stem cell biology is underlined by the large number of transcription factor genes that play key roles in normal stem cells, yet their disruption forms part of the pathogenesis of hematologic malignancies.[43] However, relatively little is known about the regulation of many of these key regulators and less still about the way they interact with each other in forming the transcriptional networks controlling hematopoiesis.

Scl occupies a central position in HSC regulatory cascades. Activation of *Scl* expression accompanies the formation of the hemangioblast,[44,45] whereas ectopic expression of *scl* in zebrafish embryos results in excessive hemangioblast formation.[46] In addition, *Scl* is required for the generation of HSCs.[6,7] Extensive dissection of the murine *Scl* locus has led to the identification of several cis-regulatory elements that direct Scl expression in vivo to the hemangioblast, hemopoietic progenitors, and differentiated cells and to endothelial progeny.[47-51] Taken together, this work characterizing the upstream regulation of *Scl* suggests that Scl functions as a nodal point for the integration of signals responsible for establishing the transcriptional program for HSC development. However, the downstream Scl target genes that transmit this

A

B
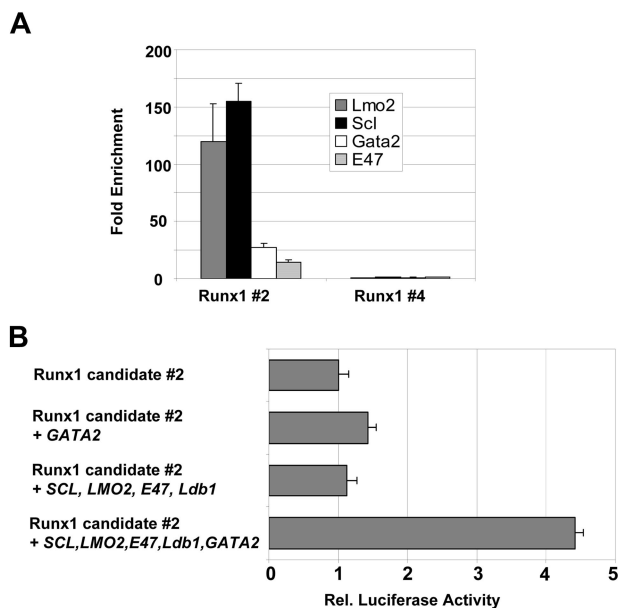
Figure 7. The SCL/Lmo2/Gata-2 complex binds to and activates *Runx1* and *Runx3*. Real-time PCR analysis of 416B ChIP material showing enrichment for the *Runx1* #2 (A) candidate element. *Runx1* #4 region was included as a negative control (B). The *Runx1* #2 element can be transactivated by a multiprotein complex containing SCL, LMO2, E47, Ldb1, and GATA2. Transactivation assays were performed in Cos cells as described in "Transactivation assay" and were internally controlled by cotransfection of pEF-BOS-lacZ. Error bars represent SD.

information remain, for the most part, uncharacterized. To date, only a handful of direct Scl target genes have been identified,[14,15,52-55] with only 2, *c-kit* and *Gata2*, having a known function in HSCs. Moreover, it has been suggested that Scl binds to the *c-kit* promoter as part of a repressive complex[15] and the *Gata2* regulatory element bound by SCL is an endothelial enhancer.[53] In addition and unlike Scl and Runx1,[56] neither *c-kit* nor *Gata2* is required for the formation of definitive hematopoietic cells.[57,58] Consequently, none of the Scl target genes known before this study fully explains key aspects of the early embryonic *Scl*^{−/−} phenotype nor do they directly address the issue of downstream genes important for the formation of HSCs. To identify on a genome-wide basis Scl target genes, we have generated a novel *Scl*^{−/−} YS cell line. We have determined by microarray analysis genes that are up-regulated after the reintroduction of Scl protein and have confirmed direct binding of Scl to these potential target genes by ChIP. Our approach has allowed us to identify 2 new Scl target genes, *Runx1* and *Runx3*.

The *Runx* genes encode conserved transcription factors that play vital roles in major developmental pathways.[59] In mammals, the Runx family consists of 3 known members that recognize and bind the same DNA sequence motif (ACCRCA) but differ in their expression pattern. In early development, *Runx1* is expressed in hematopoietic cells in the YS and fetal liver.[5,60] *Runx1* is also found in the AGM region where it is thought to regulate the emergence of hematopoietic stem cells.[61] Correlating well with its expression pattern, knockout studies have shown *Runx1* to be essential for definitive hematopoiesis as the mutant mice lack definitive hematopoietic progenitors in both the YS and fetal liver.[36,37] *Runx3* has been shown to have important functions in diverse biologic pathways, such as transforming growth factor-beta signaling,[62,63] neurogenesis,[64,65] and T-cell development.[66,67] Morpholino-depletion analysis of *runx3* in zebrafish has suggested an important role for *runx3* in the maintenance of primitive blood and the establish-

ment of definite hematopoiesis.[38] Within the hematopoietic compartment, the expression of *Runx1* and *Runx3* overlaps in some tissues, such as the fetal liver and thymus, suggesting a degree of overlap in their transcriptional control.

The mammalian *Runx* genes share many structural elements at the genomic level, including the use of dual promoters. Each of the 3 genes is transcribed by distal and proximal promoter regions.[39] Transcription from these alternative promoters appears to be regulated by retinoids and cytokines, such as those in the TFG-β pathway.[68] In addition, *Runx* genes likely undergo some form of auto- and/or cross-regulation.[69] However, until now, very little was known with regards to the identity of other transcription factors that regulate the expression of the *Runx* genes. Scl and lmo2 had been shown to act upstream of *runx1* in the transcriptional cascade controlling zebrafish blood development.[11,70] However, these studies did not address whether *runx1* was a direct target of scl and lmo2 in the posterior lateral plate mesoderm, the fish equivalent of the AGM region. We now report that the distal P1 promoter of *Runx3* and an intronic enhancer of *Runx1* are bound by scl in vivo in hematopoietic tissues. Moreover, our work implies that *Runx1* is regulated by Scl as part of a complex containing Lmo2 and Gata2. Interestingly, an independent search for *Runx1* regulatory elements, performed by surveying DNaseI hypersensitive sites within the *Runx1* gene locus, showed that the region encompassing conserved E-box 2 is in an open chromatin configuration. Furthermore, when assayed in transgenic mice, the region spanning E-box 2 in *Runx1* was found to drive expression of a linked *lacZ* reporter gene in HSCs in the AGM and fetal liver.[24]

Transcriptional networks often contain a small number of so-called hubs, highly connected key regulatory genes. *Scl* and *Runx1* represent 2 hubs of the regulatory network controlling HSC development, and the current study provides a direct link between these 2 key regulators. We have recently shown how activity of *Runx1* can be modulated by the BMP signaling pathway.[17] Future identification of the signaling pathways that control *Scl* expression will be important to define the regulatory cascade leading from mesoderm commitment to HSC specification. Lastly, given the observation that overexpression of *Scl* increases HSC long-term repopulating activity,[71] the TAT-Scl fusion protein generated here may be a useful nonretroviral tool to achieve transient in vitro amplification of HSCs in the context of clinical applications, such as cord blood and bone marrow transplantations.

Authorship

Correspondence: Berthold Göttgens, Department of Haematology, Cambridge Institute for Medical Research, Cambridge University, Hills Road, Cambridge, CB2 0XY, United Kingdom; e-mail: bg200@cam.ac.uk.

References

1. McGrath KE, Palis J. Hematopoiesis in the yolk sac: more than meets the eye. Exp Hematol. 2005;33:1021-1028.

2. Palis J, Yoder MC. Yolk-sac hematopoiesis: the first blood cells of mouse and man. Exp Hematol. 2001;29:927-936.

3. Medvinsky A, Dzierzak E. Definitive hematopoiesis is autonomously initiated by the AGM region. Cell. 1996;86:897-906.

4. Kumaravelu P, Hook L, Morrison AM, et al. Quantitative developmental anatomy of definitive haematopoietic stem cells/long-term repopulating units (HSC/RUs): role of the aorta-gonad-mesonephros (AGM) region and the yolk sac in colonisation of the mouse embryonic liver. Development. 2002;129:4891-4899.

5. Samokhvalov IM, Samokhvalova NI, Nishikawa S. Cell tracing shows the contribution of the yolk sac to adult haematopoiesis. Nature. 2007;446: 1056-1061.

6. Robb L, Lyons I, Li R, et al. Absence of yolk sac hematopoiesis from mice with a targeted disruption of the scl gene. Proc Natl Acad Sci U S A. 1995;92:7075-7079.

7. Shivdasani RA, Mayer EL, Orkin SH. Absence of blood formation in mice lacking the T-cell leukaemia oncoprotein tal-1/SCL. Nature. 1995;373: 432-434.

8. Visvader JE, Fujiwara Y, Orkin SH. Unsuspected role for the T-cell leukemia protein SCL/tal-1 in vascular development. Genes Dev. 1998;12:473-479.

9. Warren AJ, Colledge WH, Carlton MB, Evans MJ, Smith AJ, Rabbitts TH. The oncogenic cysteine-rich LIM domain protein rbtn2 is essential for erythroid development. Cell. 1994;78:45-57.

10. Yamada Y, Pannell R, Forster A, Rabbitts TH. The oncogenic LIM-only transcription factor Lmo2 regulates angiogenesis but not vasculogenesis in mice. Proc Natl Acad Sci U S A. 2000;97:320-324.

11. Patterson LJ, Gering M, Eckfeldt CE, et al. The transcription factors Scl and Lmo2 act together during development of the hemangioblast in zebrafish. Blood. 2007;109:2389-2398.

12. Wadman IA, Osada H, Grutz GG, et al. The LIM-only protein Lmo2 is a bridging molecule assembling an erythroid, DNA-binding complex which includes the TAL1, E47, GATA-1 and Ldb1/NLI proteins. EMBO J. 1997;16:3145-3157.

13. Anguita E, Hughes J, Heyworth C, Blobel GA, Wood WG, Higgs DR. Globin gene activation during haemopoiesis is driven by protein complexes nucleated by GATA-1 and GATA-2. EMBO J. 2004;23:2841-2852.

14. Lecuyer E, Herblot S, Saint-Denis M, et al. The SCL complex regulates c-kit expression in hematopoietic cells through functional interaction with Sp1. Blood. 2002;100:2430-2440.

15. Vitelli L, Condorelli G, Lulli V, et al. A pentamer transcriptional complex including tal-1 and retinoblastoma protein downmodulates c-kit expression in normal erythroblasts. Mol Cell Biol. 2000;20: 5330-5342.

16. Palomero T, Odom DT, O'Neil J, et al. Transcriptional regulatory networks downstream of TAL1/SCL in T-cell acute lymphoblastic leukemia. Blood. 2006;108:986-992.

17. Pimanda JE, Donaldson IJ, de Bruijn MF, et al. The SCL transcriptional network and BMP signaling pathway interact to regulate RUNX1 activity. Proc Natl Acad Sci U S A. 2007;104:840-845.

18. Choi K, Kennedy M, Kazarov A, Papadimitriou JC, Keller G. A common precursor for hematopoietic and endothelial cells. Development. 1998; 125:725-732.

19. Thalmeier K, Meissner P, Reisbach G, Falk M, Brechtel A, Dormer P. Establishment of two permanent human bone marrow stromal cell lines with long-term post irradiation feeder capacity. Blood. 1994;83:1799-1807.

20. Ottersbach K, Dzierzak E. The murine placenta contains hematopoietic stem cells within the vascular labyrinth region. Dev Cell. 2005;8:377-387.

21. Peitz M, Pfannkuche K, Rajewsky K, Edenhofer F. Ability of the hydrophobic FGF and basic TAT peptides to promote cellular uptake of recombinant Cre recombinase: a tool for efficient genetic engineering of mammalian genomes. Proc Natl Acad Sci U S A. 2002;99:4489-4494.

22. Donaldson IJ, Gottgens B. CoMoDis: composite motif discovery in mammalian genomes. Nucleic Acids Res. 2007;35:e1.

23. Forsberg EC, Downs KM, Bresnick EH. Direct interaction of NF-E2 with hypersensitive site 2 of the beta-globin locus control region in living cells. Blood. 2000;96:334-339.

24. Nottingham WT, Jarratt A, Burgess M, et al. Runx1-mediated hematopoietic stem cell emergence is controlled by a Gata/Ets/SCL-regulated enhancer. Blood. 2007;110:4188-4197.

25. Klotz L, Dani I, Edenhofer F, et al. Peroxisome proliferator-activated receptor gamma control of dendritic cell function contributes to development of CD4+ T cell anergy. J Immunol. 2007;178: 2122-2131.

26. Krosl J, Austin P, Beslu N, Kroon E, Humphries RK, Sauvageau G. In vitro expansion of hematopoietic stem cells by recombinant TAT-HOXB4 protein. Nat Med. 2003;9:1428-1432.

27. Nolden L, Edenhofer F, Haupt S, et al. Site-specific recombination in human embryonic stem cells induced by cell-permeant Cre recombinase. Nat Methods. 2006;3:461-467.

28. Porcher C, Liao EC, Fujiwara Y, Zon LI, Orkin SH. Specification of hematopoietic and vascular development by the bHLH transcription factor SCL without direct DNA binding. Development. 1999; 126:4603-4615.

29. Doyle S, Vaidya S, O'Connell R, et al. IRF3 mediates a TLR3/TLR4-specific antiviral gene program. Immunity. 2002;17:251-263.

30. Lund S, Christensen KV, Hedtjarn M, et al. The dynamics of the LPS triggered inflammatory response of murine microglia under different culture and in vivo conditions. J Neuroimmunol. 2006; 180:71-87.

31. Magder S, Neculcea J, Neculcea V, Sladek R. Lipopolysaccharide and TNF-alpha produce very similar changes in gene expression in human endothelial cells. J Vasc Res. 2006;43:447-461.

32. Saban MR, Hellmich H, Nguyen NB, Winston J, Hammond TG, Saban R. Time course of LPS-induced gene expression in a mouse model of

genitourinary inflammation. Physiol Genomics. 2001;5:147-160.

33. Saban MR, Saban R, Hammond TG, et al. LPS-sensory peptide communication in experimental cystitis. Am J Physiol Renal Physiol. 2002;282: F202-F210.

34. Sharif O, Bolshakov VN, Raines S, Newham P, Perkins ND. Transcriptional profiling of the LPS induced NF-kappaB response in macrophages. BMC Immunol. 2007;8:1.

35. Donaldson IJ, Chapman M, Kinston S, et al. Genome-wide identification of cis-regulatory sequences controlling blood and endothelial development. Hum Mol Genet. 2005;14:595-601.

36. Okuda T, van Deursen J, Hiebert SW, Grosveld G, Downing JR. AML1, the target of multiple chromosomal translocations in human leukemia, is essential for normal fetal liver hematopoiesis. Cell. 1996;84:321-330.

37. Wang Q, Stacy T, Binder M, Marin-Padilla M, Sharpe AH, Speck NA. Disruption of the Cbfa2 gene causes necrosis and hemorrhaging in the central nervous system and blocks definitive hematopoiesis. Proc Natl Acad Sci U S A. 1996;93: 3444-3449.

38. Kalev-Zylinska ML, Horsfield JA, Flores MV, et al. Runx3 is required for hematopoietic development in zebrafish. Dev Dyn. 2003;228:323-336.

39. Levanon D, Groner Y. Structure and regulated expression of mammalian RUNX genes. Oncogene. 2004;23:4211-4219.

40. Cantor AB, Orkin SH. Transcriptional regulation of erythropoiesis: an affair involving multiple partners. Oncogene. 2002;21:3368-3376.

41. Enver T, Greaves M. Loops, lineage, and leukemia. Cell. 1998;94:9-12.

42. Gottgens B, Green AR. Transcriptional regulation of hematopoietic stem cells. In: Lanza HMB, Melton DA, et al, ed. Handbook of Stem Cells: Amsterdam, the Netherlands: Elsevier Academic Press; 2004.

43. Tenen DG. Disruption of differentiation in human cancer: AML shows the way. Nat Rev Cancer. 2003;3:89-101.

44. Faloon P, Arentson E, Kazarov A, et al. Basic fibroblast growth factor positively regulates hematopoietic development. Development. 2000;127: 1931-1941.

45. Robertson SM, Kennedy M, Shannon JM, Keller G. A transitional stage in the commitment of mesoderm to hematopoiesis requiring the transcription factor SCL/tal-1. Development. 2000;127:2447-2459.

46. Gering M, Rodaway AR, Gottgens B, Patient RK, Green AR. The SCL gene specifies hemangioblast development from early mesoderm. EMBO J. 1998;17:4029-4045.

47. Gottgens B, Broccardo C, Sanchez MJ, et al. The scl +18/19 stem cell enhancer is not required for hematopoiesis: identification of a 5′ bifunctional hematopoietic-endothelial enhancer bound by Fli-1 and Elf-1. Mol Cell Biol. 2004;24:1870-1883.

48. Gottgens B, Nastos A, Kinston S, et al. Establishing the transcriptional programme for blood: the SCL stem cell enhancer is regulated by a multi-protein complex containing Ets and GATA factors. EMBO J. 2002;21:3039-3050.

49. Sanchez M, Gottgens B, Sinclair AM, et al. An SCL

3′ enhancer targets developing endothelium together with embryonic and adult haematopoietic progenitors. Development. 1999;126:3891-3904.

50. Silberstein L, Sanchez MJ, Socolovsky M, et al. Transgenic analysis of the stem cell leukemia +19 stem cell enhancer in adult and embryonic hematopoietic and endothelial cells. Stem Cells. 2005;23:1378-1388.

51. Delabesse E, Ogilvy S, Chapman MA, Piltz SG, Gottgens B, Green AR. Transcriptional regulation of the SCL locus: identification of an enhancer that targets the primitive erythroid lineage in vivo. Mol Cell Biol. 2005;25:5215-5225.

52. Deleuze V, Chalhoub E, El-Hajj R, et al. TAL-1/SCL and its partners E47 and LMO2 up-regulate VE-cadherin expression in endothelial cells. Mol Cell Biol. 2007;27:2687-2697.

53. Khandekar M, Brandt W, Zhou Y, et al. A Gata2 intronic enhancer confers its pan-endothelia-specific regulation. Development. 2007;134:1703-1712.

54. Lahlil R, Lecuyer E, Herblot S, Hoang T. SCL assembles a multifactorial complex that determines glycophorin A expression. Mol Cell Biol. 2004;24:1439-1452.

55. Xu Z, Huang S, Chang LS, Agulnick AD, Brandt SJ. Identification of a TAL1 target gene reveals a positive role for the LIM domain-binding protein Ldb1 in erythroid gene expression and differentiation. Mol Cell Biol. 2003;23:7585-7599.

56. Lacaud G, Gore L, Kennedy M, et al. Runx1 is essential for hematopoietic commitment at the hemangioblast stage of development in vitro. Blood. 2002;100:458-466.

57. Tsai FY, Orkin SH. Transcription factor GATA-2 is required for proliferation/survival of early hematopoietic cells and mast cell formation, but not for erythroid and myeloid terminal differentiation. Blood. 1997;89:3636-3643.

58. Ashman LK. The biology of stem cell factor and its receptor C-kit. Int J Biochem Cell Biol. 1999;31:1037-1051.

59. Ito Y. Oncogenic potential of the RUNX gene family: overview. Oncogene. 2004;23:4198-4208.

60. North T, Gu TL, Stacy T, et al. Cbfa2 is required for the formation of intra-aortic hematopoietic clusters. Development. 1999;126:2563-2575.

61. North TE, de Bruijn MF, Stacy T, et al. Runx1 expression marks long-term repopulating hematopoietic stem cells in the midgestation mouse embryo. Immunity. 2002;16:661-672.

62. Fainaru O, Woolf E, Lotem J, et al. Runx3 regulates mouse TGF-beta-mediated dendritic cell function and its absence results in airway inflammation. EMBO J. 2004;23:969-979.

63. Shi MJ, Stavnezer J. CBF alpha3 (AML2) is induced by TGF-beta1 to bind and activate the mouse germline Ig alpha promoter. J Immunol. 1998;161:6751-6760.

64. Inoue K, Ozaki S, Shiga T, et al. Runx3 controls the axonal projection of proprioceptive dorsal root ganglion neurons. Nat Neurosci. 2002;5:946-954.

65. Levanon D, Bettoun D, Harris-Cerruti C, et al. The Runx3 transcription factor regulates development and survival of TrkC dorsal root ganglia neurons. EMBO J. 2002;21:3454-3463.

66. Taniuchi I, Osato M, Egawa T, et al. Differential requirements for Runx proteins in CD4 repression and epigenetic silencing during T lymphocyte development. Cell. 2002;111:621-633.

67. Woolf E, Xiao C, Fainaru O, et al. Runx3 and Runx1 are required for CD8 T cell development during thymopoiesis. Proc Natl Acad Sci U S A. 2003;100:7731-7736.

68. Otto F, Lubbert M, Stock M. Upstream and downstream targets of RUNX proteins. J Cell Biochem. 2003;89:9-18.

69. Spender LC, Whiteman HJ, Karstegl CE, Farrell PJ. Transcriptional cross-regulation of RUNX1 by RUNX3 in human B cells. Oncogene. 2005;24:1873-1881.

70. Patterson LJ, Gering M, Patient R. Scl is required for dorsal aorta as well as blood formation in zebrafish embryos. Blood. 2005;105:3502-3511.

71. Reynaud D, Ravet E, Titeux M, et al. SCL/TAL1 expression level regulates human hematopoietic stem cell self-renewal and engraftment. Blood. 2005;106:2318-2328.

72. Huss R, Heil M, Moosmann S, et al. Improved arteriogenesis with simultaneous skeletal muscle repair in ischemic tissue by SCL(+) multipotent adult progenitor cell clones from peripheral blood. J Vasc Res. 2004;41:422-431.